

Article

A Novel Highly Sensitive Chemiluminescence Enzyme Immunoassay with Signal Enhancement Using Horseradish Peroxidase-Luminol-Hydrogen Peroxide Reaction for the Quantitation of Monoclonal Antibodies Used for Cancer Immunotherapy

Ibrahim A. Darwish * , Nourah Z. Alzoman * and Nehal N. Khalil

Department of Pharmaceutical Chemistry, College of Pharmacy, King Saud University, P.O. Box 2457, Riyadh 11451, Saudi Arabia

* Correspondence: idarwish@ksu.edu.sa (I.A.D.); nalzoman@ksu.edu.sa (N.Z.A.); Tel.: +966-114677348 (I.A.D.); Fax: +966-114676220 (I.A.D.)

Abstract: The development and validation of a novel enhanced chemiluminescence enzyme immunoassay (CLEIA) with excellent sensitivity for the quantification of monoclonal antibodies (mAbs) used for immunotherapy of cancer are described in this paper for the first time. The 96-microwell plates were used for the assay procedures, which involved the non-competitive binding reaction to a specific antigen. The immune complex of the antigen-mAb formed on the internal surface of the plate wells was quantified by a novel chemiluminescence (CL)-producing horseradish peroxidase (HRP) reaction. The reaction employed 4-(imidazol-1-yl)phenol (IMP) as a highly potent signal enhancer for the HRP-luminol-hydrogen peroxide (H_2O_2) CL reaction. The proposed CLEIA was developed for bevacizumab (BEV), as a representative example for mAbs. The CLEIA was validated in accordance with the immunoassay validation for bioanalysis standards, and all of the validation criteria were met. The assay's limit of detection (LOD) and limit of quantitation (LOQ) were 9.3 and 28.2 pg mL^{-1} , respectively, with a working dynamic range of 10–400 pg mL^{-1} . The assay enables the accurate and precise quantitation of mAbs in human plasma samples without any interference from endogenous substances and/or plasma matrix. The novel CLEIA was compared in terms of dynamic range and sensitivity with other pre-validated enzyme-linked immunosorbent assay (ELISA) using HRP/colorimetric substrate as a detection system and the observed differences were explained. The CLEIA protocol's ease of use, high throughput, and simplicity allows to analyze numerous samples in clinical settings. The proposed CLEIA has a significant benefit in the assessment of mAbs in clinical settings for the evaluation of their pharmacokinetics, pharmacodynamics, therapeutic drug monitoring, and refining their safety profiles, opening a new era for a better understanding of pharmacodynamics at the cellular level.

Keywords: cancer immunotherapy; monoclonal antibodies; chemiluminescence enzyme immunoassay; horseradish peroxidase; luminol-hydrogen peroxide system



Citation: Darwish, I.A.; Alzoman, N.Z.; Khalil, N.N. A Novel Highly Sensitive Chemiluminescence Enzyme Immunoassay with Signal Enhancement Using Horseradish Peroxidase-Luminol-Hydrogen Peroxide Reaction for the Quantitation of Monoclonal Antibodies Used for Cancer Immunotherapy. *Chemosensors* **2023**, *11*, 245. <https://doi.org/10.3390/chemosensors11040245>

Academic Editor: Yoav Broza

Received: 24 February 2023

Revised: 13 April 2023

Accepted: 13 April 2023

Published: 14 April 2023



Copyright: © 2023 by the authors. Licensee MDPI, Basel, Switzerland. This article is an open access article distributed under the terms and conditions of the Creative Commons Attribution (CC BY) license (<https://creativecommons.org/licenses/by/4.0/>).

1. Introduction

Immunotherapy is a very efficient approach in the treatment of different types/stages of cancer [1–3]. The most important and promising medicines used for immunotherapy of cancer are human/or humanized monoclonal antibodies (mAbs). These mAbs can promote/assist the immune system of the human body in identifying and striking cancer cells [4–6]. These mAbs can offer better features and advantages over the small chemotherapeutic molecules, e.g., tyrosine kinase inhibitors, etc., in regard to pharmacokinetic, pharmacodynamic properties and the induction of side effects. Therefore, the generation and manufacturing of therapeutic mAbs has come to represent one of the most growing

fields attracting the attraction of pharmaceutical/biotechnological industries [7–10]. The Food and Drug Administration (FDA) has approved more than 20 mAbs so far for use in the immunotherapy of various malignancies. [11]. The therapeutic benefits of most mAbs depend on their pharmacokinetic profiles which are not linear. This pattern is partly due to the neonatal Fc receptor which acts in the catabolism of mAbs before reaching the blood stream and binding to their targets [12–15]. Therefore, a closer monitoring of their plasma levels during therapy is necessary.

For the bioanalysis of therapeutic mAbs, liquid chromatography-tandem mass spectrometry (LC-MS/MS) methods with adequate sensitivity have been developed [16–20]. However, these methods suffer from many major drawbacks. These drawbacks include the time-consuming procedures used for the purification of the complex sample matrices, length of procedures for digestion by trypsin, and lack of a clear strategy to develop the proper LC-MS/MS method. Furthermore, LC-MS/MS instruments are cost-intensive, and thus not available in most clinical laboratories, especially those in poor third-world countries. These drawbacks limit the wide use of the technique in clinical laboratories. Several approaches have been developed to overcome these drawbacks, such as making the samples trypsin digestion and purification procedures simpler and faster [17–19]. However, many challenges in sample preparation remain. These challenges include the denaturation, reduction, and alkylation of mAbs before the digestion process. Furthermore, some of the LC-MS/MS methods suffer from the inconsistency of the peaks [20], poor precision of the results, and the time-intensive analysis protocol [21,22].

Basically, immunoassays represent a potentially endorsed alternative technique for the bioanalysis of mAbs by virtue of their intrinsic high specificity, sensitivity, and through-put analysis in clinical laboratories [23]. Different immunoassay platforms have been developed for the bioanalysis of mAbs. Beer et al. [24] described a flow cytometry-based microsphere immunoassay for the quantitation of mAb concentrations in human vitreous humor [24]. However, the results of the assay were imprecise owing to the use of microspheres suspension to carry out the binding reaction. Recently, our laboratory developed an automated flow-based immunoassay for the bioanalysis of therapeutic mAbs by interfacing their immune reaction to the KinExA™ 3200 biosensor [25]. The results of the assay were precise. However, the KinExA™ 3200 biosensor is not a common instrument in most clinical laboratories. Plate-based enzyme-linked immunosorbent assays (ELISAs) represent a better alternative approach for the bioanalysis of mAbs, and accordingly, different ELISAs have been developed for mAbs [26–31]. Most of these ELISAs relied on the immobilization of anti-idiotypic antibodies for capturing the mAbs from their sample solutions. This approach, as expected, gave false positive results because of the non-specific binding of similar human IgG antibodies in the samples to the immobilized anti-idiotypic antibodies [26]. Besides, some of these assays had low precision (the coefficients of variation were >20%), poor accuracy, and limited sensitivity because they used enzymes/colorimetric substrates for detection. For these reasons, the search for new, more efficient immunoassays for the bioanalysis of therapeutic mAbs is seriously important.

In recent years, chemiluminescence enzyme immunoassays (CLEIAs) have received great attention and been applied in different fields, such as pharmacology and molecular biology [32,33]. CLEIAs have higher sensitivity and wider dynamic range over the color signal based ELISAs. In addition, CLEIAs have sensitivity as high as the radioimmunoassay, but in contrast are not hazardous to health. To the best of our knowledge, no CLEIA exists in the available literature for the bioanalysis of therapeutic mAbs. In the present study, we developed a novel enhanced CLEIA for the quantification of mAbs in plasma samples by the employment of 4-(1-imidazolyl)phenol (IMP) as a CL enhancer for the HRP-luminol-H₂O₂ reaction. There were two phases to the study's experiments. The goal of the initial investigations was to determine the ideal CL conditions in the continued presence of IMP and to adapt the ideal immunoassay techniques developed in our laboratory [27]. The CLEIA was then validated in terms of its practical usefulness, sensitivity, accuracy, precision, and specificity. The current CLEIA was established for bevacizumab (BEV) as a

model for the mAbs used in cancer immunotherapy. The assay provided higher sensitivity than any existing assay for mAbs. Accordingly, it enabled the quantitation of mAbs at concentrations much lower than the other existing assays.

2. Experimental

2.1. Instruments

Multifunctional (absorbance, fluorescence, chemiluminescence) microplate/cuvette reader (Spectramax M5: Molecular Devices, San Jose, CA, USA). Automatic microplate strip washer (MW-12A: Bio-Medical Electronics Co., Ltd., Shenzhen, China). Biofuge centrifuge (Z206A: Hermle Labortechnik, Wehingen Germany). Microprocessor laboratory pH meter (Mettler-Toledo International Inc., Zürich, Switzerland). Electric digital balance (JB1603-C/FACT: Mettler-Toledo International Inc., Zürich, Switzerland). Incubator (Sanyo MIR162: Onoda, Japan). Biocool fridge (Sanyo MPR-311D: Onoda, Japan). Vortex (Clifton cyclone CM1: Weston, UK). Biomedical freezer (Sanyo MDF-U5312: Onoda, Japan). Milli-Q water purification system (Millipore Ltd., Bedford, MA, USA).

2.2. Materials

BEV was obtained from BOC Sciences (Jersey City, NJ, USA). Recombinant human vascular epidermal growth factor receptor protein (VEGF) was purchased from R&D Systems (Lille, France). Goat anti-human HRP-IgG conjugate and bovine serum albumin (BSA) were purchased from Sigma-Aldrich Chemicals Co. (St. Louis, MO, USA). Luminol was purchased from ABCR GmbH (Karlsruhe, Germany). 4-(Imidazol-1-yl)phenol (IMP) was purchased from Sigma-Aldrich Chemicals Co. (St. Louis City, MO, USA). Hydrogen peroxide was purchased from Merck (Jersey City, NJ, USA). White opaque flat-bottom high binding 96-well plates for chemiluminescence were purchased from Corning/Costar Inc. (Corning, NY, USA). King Khalid University Hospital in Riyadh, Kingdom of Saudi Arabia provided human plasma samples, which were stored frozen at $-20\text{ }^{\circ}\text{C}$ until they were utilized in the experiment. All other chemical/reagents and buffer components used throughout the work were of analytical grade.

2.3. Buffer Solutions

Carbonate buffer (50 mM, pH 9.6) was used as coating buffer of VEGF protein onto the assay wells. Phosphate buffer saline (PBS) solution (0.1 mM, pH 7.4) was utilized for binding of BEV and HRP-IgG conjugate to the assay plate wells. PBS containing Tween-20 (PBS-T; 0.05%, *v/v*) was used for washing the wells of the assay plates. The wells of the assay plates were blocked using PBS containing BSA (2%, *w/v*). Britton-Robinson buffer solution of varying pH values (6–6.5 and 9.5–11) was prepared. The solution consisted of 0.0286 M citric acid, 0.0286 M monopotassium phosphate, 0.0286 M boric acid, and 0.0286 M and 0.0286 M hydrochloric acid, and the pH values were adjusted to the desired values with 0.2 M sodium hydroxide. Details of the preparation of these buffer solutions were described in our previous study [27]. Tris-HCl buffer (0.1 M, pH 8.5) was prepared by dissolving 12.1 g of tris(hydroxymethyl)aminomethane hydrochloride in approximately 800 mL water, the pH was adjusted to 8.5, and the buffer solution was completed to 1 L with water. Tris-HCl buffer was used for the CL-producing reaction.

2.4. Solutions of BEV and VEGF

By reconstituting 5 mg of the lyophilized substance in 5 mL PBS, the stock solution of BEV (1 mg mL^{-1}) was obtained. The working solution ($1\text{ }\mu\text{g mL}^{-1}$) was carefully prepared by appropriately diluting the stock solution in PBS. The stock solution was kept at $-20\text{ }^{\circ}\text{C}$ and the working solution was kept at $4\text{ }^{\circ}\text{C}$ until use.

The stock solution of VEGF ($100\text{ }\mu\text{g mL}^{-1}$) was prepared, as per the supplier instructions, by reconstituting an accurate amount (0.5 mg) of the lyophilized protein in PBS containing BSA (0.1%, *w/v*). Until usage, the solution was kept frozen at $-20\text{ }^{\circ}\text{C}$. The

stock solution of VEGF was diluted in the carbonate buffer to create the working solution ($50 \mu\text{g mL}^{-1}$). The solutions were kept refrigerated at 4°C until use.

2.5. Enhanced Chemiluminescence Solution

A freshly prepared enhanced chemiluminescence solution (ECS) was prepared in Tris-HCl buffer (0.1 M, pH 8.5). The ECS consisted of luminol (0.1 mM), hydrogen peroxide (1 mM), and IMP (0.2 mM).

2.6. CLEIA Procedures and Data Analysis

By incubating $50 \mu\text{L}$ of the solution ($1 \mu\text{g mL}^{-1}$) in the carbonate buffer solution for 1 h at 37°C in a thermostatically controlled incubator, VEGF protein was passively coated onto the internal surface of the microwells of 96-well high-binding white opaque plates. The washing buffer solution was used to wash the plate wells three times (PBS-T). By allowing $100 \mu\text{L}$ of blocking buffer solution (BSA, 2% *w/v* in PBS) to sit in the wells of the assay plates for 0.5 h at 37°C , the remaining protein-binding sites on the wells were blocked. The plate was then cleaned with PBS-T three times. In each well of the test plates, aliquots ($50 \mu\text{L}$) of the standard solution of BEV or BEV-spiked plasma samples were added. The binding of BEV to the immobilized antigen (VEGF) was allowed to proceed for 0.5 h at 37°C . The wells were washed 3 times with PBS-T, and $50 \mu\text{L}$ of the secondary enzyme-labelled antibody (HRP-IgG) solution (diluted 1:5000 in PBS) was added to each well. At room temperature ($25 \pm 2^\circ\text{C}$), HRP-IgG binding to the immunological complex (mAb-antigen protein) was permitted to continue for one hour. After three PBS-T washes, $200 \mu\text{L}$ of the CL substrate solution was applied to the plate wells. The microplate reader assessed the CL intensities at 425 nm after allowing the luminol activation reaction and CL development to run for 60 s at room temperature. The data were acquired using Spectramax[®] software (Spectramax M5: Molecular Devices, CA, USA) and transformed to Microsoft Excel 2016 (Microsoft Corporation, Washington, DC, USA) for fitting. The calibration curve was constructed by plotting the CL intensities (as arbitrary units: AU) versus the corresponding concentrations of BEV calibrator solutions. Concentrations of BEV in the plasma samples were then derived by the linear regression equation.

3. Results and Discussion

3.1. Strategy for CLEIA Development

mAbs are very important in the immunotherapy of different types of cancers [34]. However, the patent rights of some currently used mAbs have already expired [35,36] while those of others will expire in near future [37]. Expectedly, biosimilars and/or bio-better versions of these mAbs will be produced by many pharmaceutical companies. Therefore, characterization and bioanalysis for the original drugs and their biosimilar products would be necessary. Accordingly, there will be a serious need for a proper analytical tool for the assessment of the pharmacokinetic parameters in bioequivalence studies for these drugs and their therapeutic monitoring during therapy. The patent rights of BEV have recently expired [35] and its biosimilars have started to be introduced. Due to these considerations, BEV was chosen as the representative target analyte in the construction of the CLEIA detailed in this article. BEV exerts its immunotherapeutic actions via the binding to VEGF [38]. Therefore, VEGF was chosen as an antigen for the capturing of BEV in the construction of the suggested CLEIA. Many different immunoassay formats can be employed in the development of the present CLEIA [39]. In previous studies [27,28], our laboratory developed a non-competitive format-based ELISA for mAbs by using HRP/colorimetric substrate for detection, and the results confirmed the reliability of the format [27]. Therefore, this format was considered in this study. Since BEV is a mAb of IgG subtype, anti-human IgG (whole molecules) conjugated with HRP enzyme was considered to reveal the binding BEV to VEGF. The selection was also supported by our previous study which demonstrated the successful use of HRP/colorimetric substrate in the development of ELISA for BEV [27]. Besides, HRP is the enzyme that has gained the greatest significance in the development

of very sensitive CLEIAs. The intensity of HRP-based CL can be significantly enhanced by several hundred/thousand folds upon the addition of another molecule as a CL enhancer. A variety of compounds have been used as signal enhancers in the development of CLEIAs [40]. Enhanced chemiluminescent reactions mostly yield more intense, longer lasting, and more stable light emission. The detection of numerous substances has been carried out using this improved CL technique [41–43]. Previous studies revealed that the use of 4-(imidazol-1-yl)phenol (IMP) as a CL enhancer provided more intense, prolonged, and stable light emissions in developing CLEIA [44]. For these reasons, the HRP-luminol-H₂O₂-IMP reaction was considered for its employment as a detection system in the CLEIA described herein.

3.2. Description and Optimization of CLEIA

In the current study, a novel CLEIA for mAbs used in cancer immunotherapy is described. Bevacizumab (BEV) is used as a representative example. Figure 1 illustrates the general protocol of this CLEIA which is carried out in four steps: (A) immobilization of the antigen (VEGF) onto internal surface of the assay plate and blocking the remaining protein-binding sites existing on the surface of the wells with high concentration of BSA solution; (B) binding of mAb (BEV) with its corresponding antigen (VEGF) that has been coated onto the microwells of the assay plates; (C) binding of HRP-IgG to the antigen-mAb complex formed onto the assay plate wells; (D) carrying out the enhanced CL-inducing reaction by adding the CL substrate solution. The plate reader recorded the CL signals at 425 nm. The concentrations of the mAb in the sample solutions were correlated with the observed signals.

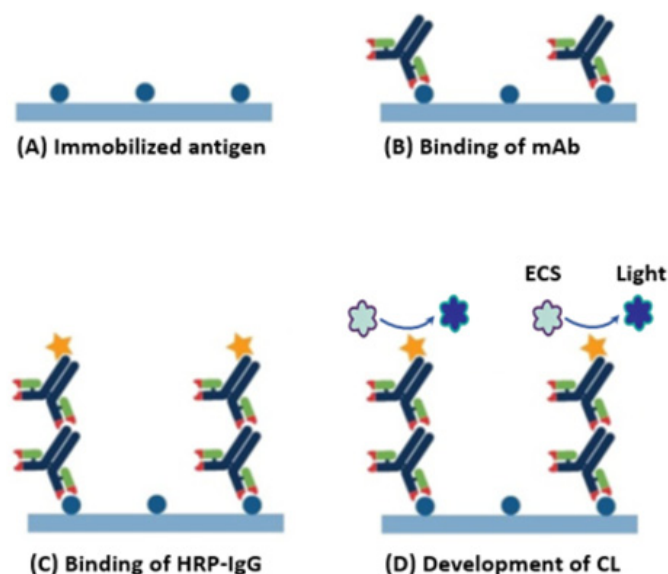


Figure 1. Illustrative diagram of the CLEIA for mAbs. (A) the antigen (VEGF) is immobilized onto the inner surface of the microwells of the assay plate and blocked with BSA. (B) binding of mAb (BEV) to the immobilized VEGF. (C) binding of HRP-IgG to the antigen-mAb complex. (D) development of CL by the HRP-luminol-H₂O₂ reaction using the IMP as a CL enhancer. Abbreviations were: CLEIA, chemiluminescence enzyme immunoassay; mAb, monoclonal antibody; VEGF, epidermal growth factor receptor; BSA, bovine serum albumin; BEV, bevacizumab; IMP, 4-(imidazol-1-yl)phenol.

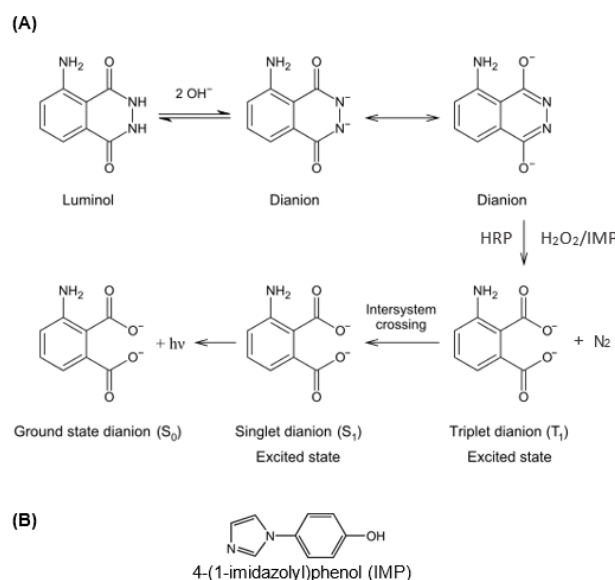
In our prior study [27], we optimized the settings for the binding of VEGF antigen, blocking of the assay plate, binding of BEV mAb, and binding of HRP-IgG, which are all listed in Table 1. In this study, the factors influencing the improved HRP-based CL-inducing reaction are adjusted. The impacts of various parameters determining the reaction's CL intensity are discussed in the sections that follow.

Table 1. A summary for the optimized parameters/conditions of the binding reactions used for development of the proposed CLEIA for BEV.

Parameter/Condition	Optimum Value
Antigen protein	VEGF
Antigen concentration ($\mu\text{g mL}^{-1}$)	1
Coating time (h)/temperature ($^{\circ}\text{C}$)	0.5/37
Blocking with BSA: time (h)/temperature ($^{\circ}\text{C}$)	0.5/37
Binding of mAb: time (h)/temperature ($^{\circ}\text{C}$)	0.5/37
Enzyme-IgG conjugate	HRP-IgG
Dilution of HRP-IgG (fold)	5000
Binding of HRP-IgG: time (h)/temperature ($^{\circ}\text{C}$)	0.5/25

3.2.1. Chemiluminescence Reaction

HRP catalyzes the reaction between luminol (as a hydrogen donor) and hydrogen peroxide (H_2O_2 , as an oxidant and hydrogen acceptor). The excited-state oxidation product decays during the oxidation of luminol, which results in the emission of light energy (CL). In the presence of IMP acting as a CL enhancer, the intensity of the transmitted CL is increased. The chemical composition of IMP and the mechanism of the increased HRP-luminol- H_2O_2 reaction are both provided in Figure 2. It is believed that the primary cause of the CL promotive effect caused by the electron transfer between luminol, and radicals was the production of the phenoxyl radical of IMP. Based on earlier research with other 4-substituted phenols [45], we hypothesized that the electronic properties of the substituents, specifically the magnitude of the resonance effect, play a crucial role in radical stabilization and, consequently, in the improvement of chemiluminescent intensity. The IMP's 4-substituent, which has an aromatic ring and nitrogen heteroatoms, may be able to stabilize the phenoxyl radicals through resonance via π -delocalization. Furthermore, electron-donating groups stabilize phenoxyl radicals by reducing the energy required for the O-H bond to dissociate. So, we assumed that this was the cause of IMP's ability to improve CL intensity the most effectively.

**Figure 2.** The mechanism of enhanced CL reaction-catalyzed HRP (A) and the chemical structure of 4-(1-imidazolyl)phenol (IMP) used as a CL enhancer for HRP-luminol- H_2O_2 reaction (B).

3.2.2. Effect of Concentrations of Luminol, IMP and H_2O_2

In order to evaluate the effect of the luminol on the CL intensity, different concentrations (0–0.5 mM) of luminol were prepared in the ECS containing constant concentrations of H_2O_2 and IMP (1 and 0.2 mM, respectively) of the CL intensity (as arbitrary units) was

measured for each concentration. The results (Figure 3A) demonstrated that the maximum CL intensity was obtained when the concentration of luminol was 0.1 mM.

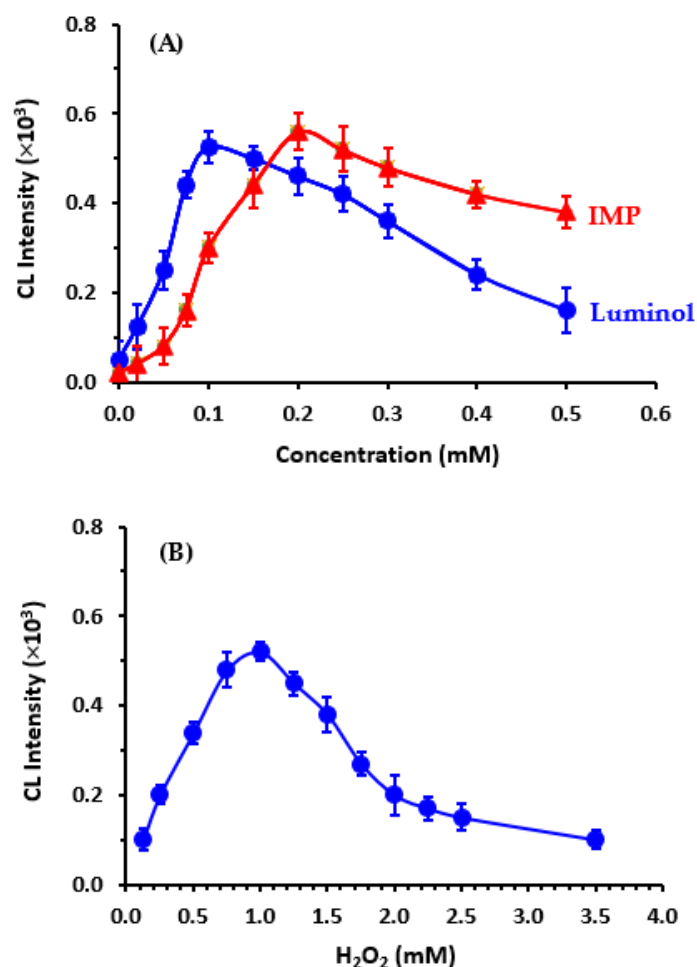


Figure 3. Effect of concentrations of luminol, IMP (A) and H_2O_2 (B) on the CL intensity induced by HRP-luminol- H_2O_2 -IMP reaction. The values are mean of 3 determinations \pm SD.

To study the impact of IMP concentration on the CL intensity, a similar set of trials were performed utilizing various concentrations (0–0.5 mM) of IMP and fixed concentrations of luminol and H_2O_2 (0.1 and 1 mM, respectively). The results (Figure 3A) demonstrated that the maximum CL intensity was obtained when the concentration of IMP was 0.2 mM. Accordingly, the concentrations of luminol and IMP used for subsequent experiments were 0.1 and 0.2 mM, respectively.

The impact of H_2O_2 concentration in ECS on the CL intensity has been studied using varying concentrations 0.1–3.5 mM of H_2O_2 , while the concentrations of luminol and IMP in the ECS were constant. It was discovered that up to 1 mM of H_2O_2 , the CL intensity increases in tandem with the increase in H_2O_2 concentrations, beyond which the CL intensity decreases (Figure 3B). According to this result, the H_2O_2 concentration used for carrying out the subsequent experiments was selected.

3.2.3. Effect of pH and Organic Solvent Content in ECS

The effect of pH of buffer solutions on the enhanced CL was tested in the range of 6–11. Britton-Robinson buffer was used for pH values of 6–6.5 and 9.5–11. However, Tris-HCl buffer was used in the range of pH values of pH 7–9. The pH values mentioned here are the pH of the buffer solution before addition of the other reagents, and these values did not change upon adding the reagents of ECS solution (luminol, H_2O_2 , and IMP) with their concentrations (Table 2). Moreover, it is wise to mention that the activity of immobilized

HRP (bound to the antigen-mAb complex) had higher stability under harsh pH conditions (acid and alkaline) compared to that of the free HRP enzymes. Therefore, the pH study described herein is focused on the CL signal generation by components other than HRP enzyme. These results revealed that the IM-HRP enzymes were more resistant to changes in the pH. The amplification of CL was carried out with luminol, H₂O₂, and IMP included. The findings (Figure 4A) showed that the pH range between 8 and 9 produced the highest CL intensity. The pH value of 8.5 was chosen for all of the studies that came after. The enhancers, including IMP, must first be pre-dissolved in an organic solvent because they are typically difficult to dissolve in aqueous CL systems. Only dimethylformamide (DMF) can dissolve IMP. Hence, the influence of DMF concentration in the ECS on the CL intensity was researched between 1% and 60%. However, when the content of DMF is greater than 10%, the effect CL intensity decreased. It was discovered that the presence of DMF in the ECS (up to 10%) had no adverse effect on the CL intensity (Figure 4B). It is widely known that IMP may precipitate in the ECS and the CL intensity will decrease if the DMF concentration in the buffer is too low. Additionally, if the amount of DMF in the ECS is too high, it might have an impact on the activity of HRP bound to the assay plate wells and reduce the CL intensity. Accordingly, the concentration of DMF used in preparing the ECS for the subsequent experiments was 2%. This concentration was adequate to avoid any precipitation for IMP in the ECS and had no harmful effect on the activity of HRP.

Table 2. Effect of ECS additives on the pH values of buffer solutions.

pH of Buffer Solution	pH of ECS Solutions
6	6
6.5	6.5
7	7
7.6	7.6
8	8
8.5	8.5
9	9
9.5	9.5
10	10
10.6	10.6
11	11

3.2.4. Effect of ECS Volume

The proper volume of ECS was adjusted through carrying out the CL-developing reaction using different volumes of the ECS (50, 100, 150 and 200 µL/well) and the CL responses were measured, and RSD of the readings were calculated. The results demonstrated that the CL intensity increased, in linear proportion, with the volume of ECS. The linear regression equation was:

$$Y = 0.005 + 0.0052X \quad (r = 0.9997)$$

where Y, X, and r are the CL intensity, volume of ECS (µL), and the linearity correlation coefficient, respectively. It was also observed that the precision of the readings, expressed as RSD values, decrease as the volume increases. These calculated RSD values were 15.15%, 11.11%, 6.1%, and 3.8% when the ECS volumes were 50, 100, 150, and 200 µL/well, respectively. In conclusion, the lowest RSD value (3.8%) was obtained when 200 µL/well was used. It wise to mention that volumes larger than 200 µL/well were not tested because the maximum volume capacity of the well of the assay plates was 250 µL. To keep the convenient manipulation of the plates, 200 µL was used. Accordingly, this volume was used in all the subsequent experiments.

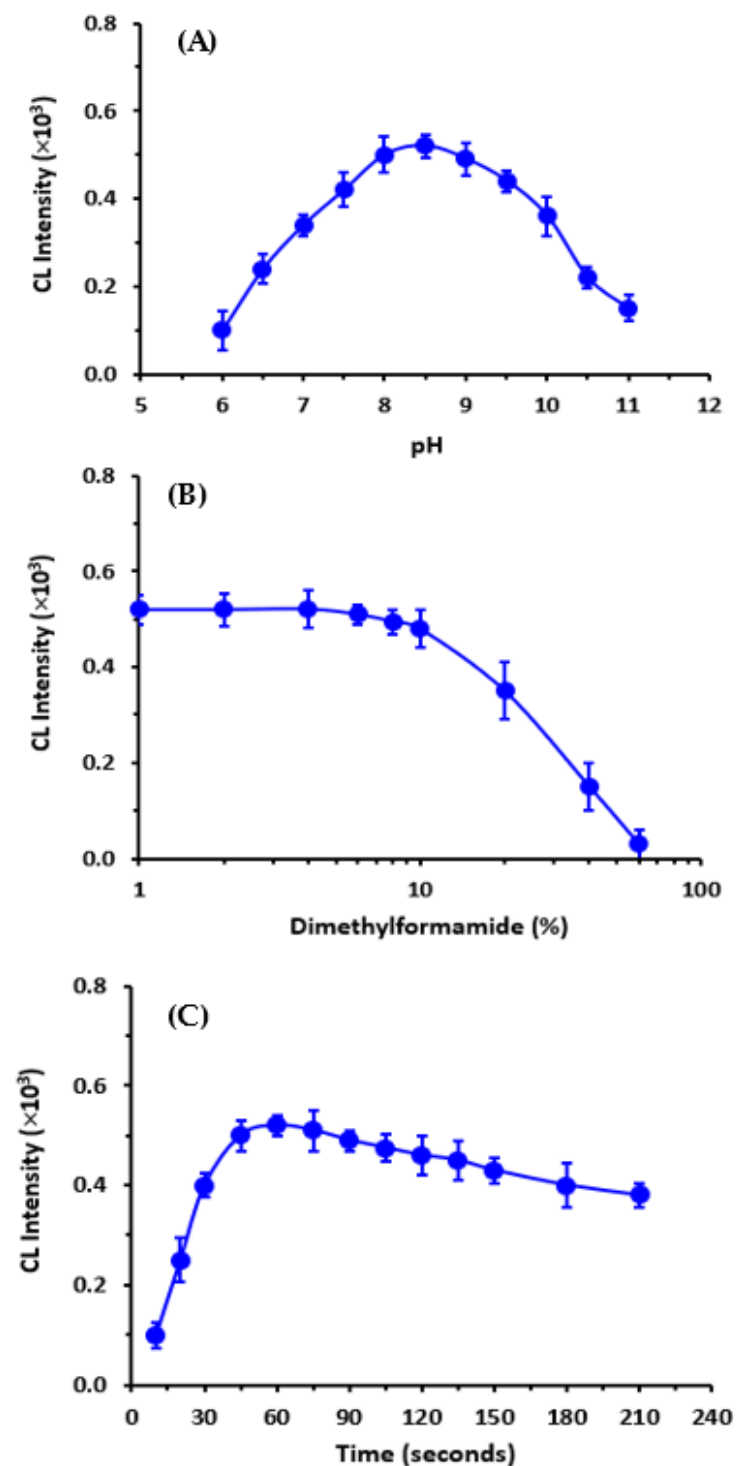


Figure 4. Effect of pH of ECS solution (A), dimethylformamide concentrations in the ECS (B) and kinetic of CL reaction (C) on the CL intensity induced by HRP-luminol- H_2O_2 -IMP reaction. The values are mean of 3 determinations \pm SD.

3.2.5. Kinetic Profile of Enhanced CL Reaction

In general, the kinetic profile of the CL-producing reaction depends on the rate of generation of the CL-emitting species and also the rate of formation of the final product [46]. The CL emission usually reaches its maximum value quickly subsequent to reaction initiation, remaining stable for a while and then declining slowly due to the decay of the species in the excited state to that of the ground state under these analytical conditions. For

construction of an assay with the highest possible sensitivity, the measurements should be performed at the time of maximum CL signal and before a significant decay. In the current work, the kinetic profile of the enhanced CL-reaction was evaluated by monitoring the CL signals for 210 s from the reaction initiation. It was found that the maximum CL signals were obtained in the time range of 45–75 s, then started to decline slowly (Figure 4C). Besides, measuring the signals at 60 s gave better reading precision (lower RSD values). In light of these findings, all future investigations assessed CL signals at 60 s.

In Table 3, an overview of the variables influencing the enhanced CL reaction utilized as the detection system in the suggested CLEIA for mAbs is provided.

Table 3. A summary for the optimization of the factors affecting the enhanced CL reaction used as detection system in the proposed CLEIA for BEV.

Parameter/Condition	Optimum Value
Luminol concentration (mM)	0.1
H ₂ O ₂ concentration (mM)	2
IMP concentration (mM)	0.2
pH of ECS (pH unit)	8.5
Concentration of DMF in ECS (% <i>v/v</i>)	2
Volume of ECS (μL/well)	200
CL development time (s)	60
CL measurement wavelength (nm)	425

3.3. Validation of the CLEIA

3.3.1. Sensitivity and Working Range

Under the optimized assay protocol and enhanced CL detection system (Tables 1 and 2, respectively), standard calibrator solutions of BEV of various concentrations (0–400 pg mL⁻¹) were analyzed and the CL signals were generated. The obtained CL signals of the BEV standard solutions were correlated versus their corresponding BEV concentrations and linear regression analysis of the data was carried out. It was discovered that the CL intensity linked in a good way (correlation coefficient, $r = 0.9982$) with the BEV concentrations (Figure 5A) in the range of 10–400 pg mL⁻¹. The regression equation was: $Y = 0.0284 + 0.0052X$, where Y is the CL intensity ($\times 10^3$) and X is the concentration of BEV in pg mL⁻¹. Table 4 lists the linear fitted variables that were determined.

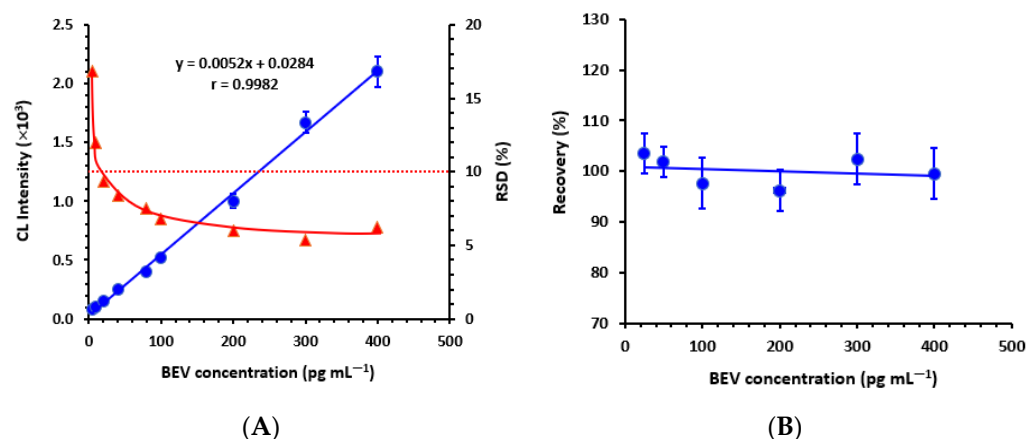


Figure 5. Panel (A) calibration curve (●) and precision profile (▲) of the proposed CLEIA for BEV. The linear fitting equation of CL intensity (left Y-axis) vs. BEV concentration (X-axis) and its correlation coefficient (r) are given on the graph. Panel (B) recovery study for analysis of diluted plasma samples containing varying concentrations of BEV by the proposed CLEIA. The presented values are mean of 3 determinations \pm SD.

Table 4. Results linear regression analysis and validation parameters of the proposed CLEIA for BEV.

Parameter	Value
Working range (pg mL ⁻¹)	10–400
Intercept	28.4
Standard deviation of intercept	14.68
Slope	5.2
Standard deviation of slope	1.4
Correlation coefficient (r)	0.9982
LOD (pg mL ⁻¹)	9.3
LOQ (pg mL ⁻¹)	28.2

According to the International Council of Harmonization's (ICH) recommendations for validating analytical techniques, the limit of detection (LOD) and limit of quantification (LOQ) of the CLEIA were established [47]. The formula utilized was as follows: LOD or LOQ = $\times SD_a/b$; Where $\times = 3.3$ for LOD and 10 for LOQ, SD_a is the standard deviation of the intercept, and b is the slope. The LOD and LOQ were found to be 9.3 and 28.2 pg mL⁻¹, respectively. This high sensitivity of the present CLEIA enables BEV quantitation in biological samples including plasma, even after ~1 million dilution fold, as the recorded average maximum concentration of BEV in plasma was 323 μ g mL⁻¹ [48].

Figure 5A displays the precision profile that was generated utilizing the calibration solution results after being examined in three repetitions. The assay's entire working range (10–400 pg mL⁻¹) had RSD% values under 10%.

3.3.2. Precision and Accuracy

By analyzing three replicates of every sample as a batch in a single assay run, the intra-assay precision of the CLEIA was assessed at various BEV concentration levels (25–300 pg mL⁻¹). Identical samples were examined as duplicates in three successive independent runs to evaluate the inter-assay precision. The assay provided satisfactory precision in accordance with the criteria for immunoassay validation [49]. The RSD was not greater than 5.2% and 6.1% for the intra-assay and inter-assay precisions, correspondingly (Table 5). We primarily credited the utilization of a high concentration of VEGF protein immobilized on the assay plate as a capture agent for BEV for the proposed CLEIA's excellent precision. This circumstance made the proposed CLEIA precision depend only on the concentrations of the BEV and HRP-based enhanced CL-producing reaction, whose ECS solution was dispensed with high precision.

Table 5. Precision and accuracy of the proposed CLEIA for BEV.

Intra-Assay Precision			Inter-Assay Precision		
Spiked Concentration (pg mL ⁻¹)	Measured Concentration (pg mL ⁻¹)	Recovery (% \pm RSD)	Spiked Concentration (pg mL ⁻¹)	Measured Concentration (pg mL ⁻¹)	Recovery (% \pm RSD)
25	25.9	103.5 \pm 5.2	25	26.4	105.4 \pm 6.1
50	50.9	101.8 \pm 3.8	50	48.4	96.8 \pm 5.7
100	97.6	97.6 \pm 3.4	100	95.7	95.7 \pm 4.8
200	192.4	96.2 \pm 3.5	200	209.6	104.8 \pm 4.2
300	313.2	104.4 \pm 4.9	300	318.6	106.2 \pm 5.4
	Mean	100.7 \pm 3.6		Mean	101.8 \pm 5.1

By measuring the recovery of different BEV concentrations (ranging from 25 to 300 pg mL⁻¹) spiked in plasma samples diluted with PBS solution, the proposed CLEIA's accuracy was evaluated. The obtained recovery values were 96.2–104.4 (with mean value of 100.7 \pm 3.6%) and 95.7–106.2 (with mean value of 101.8 \pm 5.1%) for the intra-assay and inter-assay runs, respectively (Table 5).

Such recovery values demonstrated the efficacy of the proposed CLEIA for BEV, as a representative example of mAbs, in accordance with the requirements of immunoassay validation [49].

3.3.3. Effect of Plasma Matrix

The suggested analysis was created to quantify mAbs in plasma samples. Hence, it was important to investigate how the plasma matrix affected the assay's accuracy to prevent false positives or unfavorable outcomes when the assay was applied to plasma samples. In this study, drug-free plasma samples were spiked with BEV in a concentration range which is normally present in patient's plasma, as reported in a previous study [48]. This concentration range was 10–300 $\mu\text{g mL}^{-1}$. Those samples were subjected to analysis for their BEV content after being serially diluted with PBS to get their concentrations within the planned CLEIA's working range. The matrix effect was assessed using the recovery level calculated with the calibration curve generated with standard solutions of BEV prepared PBS. The obtained recovery values as a function of their corresponding concentrations are shown in Figure 5B. It is obvious that the recovery percentage values were around 100% and the standard deviations values did not increase 10%. These results showed that the plasma matrix had no influence, either positive or negative, on the proposed CLEIA's accuracy for routine use on diluted plasma samples. It is important to note that the therapeutic concentrations of BEV in plasma have been reported to be in the range of 10–323 $\mu\text{g mL}^{-1}$ [48].

As a result, plasma samples usually containing these large concentrations (measured in μg -scale) must be diluted with PBS at a rate of about 1,000,000,000-fold in order to achieve BEV concentrations within the assay's working range (LOQ was 28.2 pg mL^{-1}). Prior to analysis, a high level of plasma dilution was necessary, which allowed the use of relatively small patient plasma samples; 1 μL of plasma was adequate for dilution with PBS for analysis by the proposed CLEIA. The use of very small plasma samples made the assay convenient when applied in clinical laboratories.

3.4. Comparison of the Proposed CLEIA with Previous ELISA

Different ELISAs with varying levels of sensitivity (different LOQ values) have been established for quantitation of BEV in different matrices [27,29]. The values of reported LOD of these ELISAs were in the range of 0.05–1.28 ng mL^{-1} . The differences in the reported achieved LOD values were due to the enzyme labels/enzyme substrates employed in the assay development. The LOD of the proposed CLEIA was 9.3 pg mL^{-1} . These data specified that the proposed CLEIA sensitivity for BEV is greater than previous immunoassays by ~138-folds. This high sensitivity can open a new era of investigations on the pharmacodynamics of mAbs on the cellular level.

Predetermined nominated doses (5–80 ng mL^{-1}) of BEV were added (spiked) to plasma samples and subsequently, these spiked samples were analyzed by the reported ELISA [27] along with the proposed CLEIA in order to assess the analytical performance of the CLEIA with the pre-validated existing ELISA. The nominated varying BEV concentrations were chosen based on the reported sensitivity level of the ELISA. Because the proposed CLEIA has much higher sensitivity than ELISA, the samples were necessarily diluted with PBS to make their concentrations in the working range of the proposed CLEIA. The concentrations measured by ELISA were plotted versus their corresponding values obtained from the proposed CLEIA. Regression analysis of the results was performed, and the results revealed the good agreement between the two methods:

$$Y = 4.0172 + 0.9232 X \quad (r = 0.9904).$$

where Y, X, and r represent the BEV concentrations measured by the proposed CLEIA (in pg mL^{-1}), BEV concentrations measured by the reported ELISA (in ng mL^{-1}), and the linearity correlation coefficient, respectively. The intercept of correlation was 4.0172, which indicates that the concentrations obtained by CLEIA are always higher by 4.0172 (pg mL^{-1}). However, this value was very low when expressed as a percentage of the higher concentra-

tions measured by ELISA (ng mL⁻¹ scale). Moreover, the good correlation coefficient (0.9904) of the equation was confirmative of the comparative accuracy of the proposed CLEIA with the pre-validated ELISA.

4. Conclusions

The development and validation of a very sensitive and selective CLEIA for the estimation of therapeutic mAbs in plasma samples were detailed in this study using BEV as a model drug. The use of IMP as a CL enhancer led to a significant improvement in the CL intensity produced by the HRP-luminol-H₂O₂ reaction, which ultimately contributed to the assay's high sensitivity by allowing for the exact and precise quantitation of BEV in plasma samples at concentrations as low as 28.2 pg mL⁻¹. Due to the assay's great sensitivity, very small plasma sample volumes (~1 µL) can be used for analysis, which may open in a new era of pharmacodynamic studies at the cellular level.

A batch of several hundred samples can be processed every day by one analyst thanks to the proposed CLEIA's methods. Due to this characteristic, the proposed CLEIA is a potent tool for the high throughput analysis of plasma samples in the study of different pharmaceutical fields, including pharmacodynamics, pharmacokinetics, and therapeutic drug monitoring during immunotherapy, as well as for evaluating the biological equivalencies in the discovery of biosimilar or biobetter mAbs. The assay was developed and validated for the study of BEV, but it may be modified to analyze any mAb as far as a particular antigen is provided, and the optimum binding conditions are established according to that particular antigen and antibody.

Author Contributions: Conceptualization, methodology, validation, formal analysis, resources, writing—review & editing, supervision, I.A.D.; investigation, visualization, data curation, N.Z.A.; investigation, data curation, validation, N.N.K. All authors have read and agreed to the published version of the manuscript.

Funding: The authors extend their appreciation to the Deputyship for Research and Innovation, Ministry of Education in Saudi Arabia for funding this research work through the project no. (IFKSURG-2-1073).

Data Availability Statement: All data are in the article.

Acknowledgments: The authors extend their appreciation to the Deputyship for Research and Innovation, Ministry of Education in Saudi Arabia for funding this research work through the project no. (IFKSURG-2-1073).

Conflicts of Interest: The authors declare no conflict of interest.

References

1. Rini, B. Future approaches in immunotherapy. *Semin. Oncol.* **2014**, *41*, S30–S40. [[CrossRef](#)] [[PubMed](#)]
2. Kirkwood, J.M.; Butterfield, L.H.; Tarhini, A.A.; Zarour, H.; Kalinski, P.; Ferrone, S. Immunotherapy of cancer in 2012. *CA Cancer J. Clin.* **2012**, *62*, 309–335. [[CrossRef](#)] [[PubMed](#)]
3. Baumeister, S.H.; Freeman, G.J.; Dranoff, G.; Sharpe, A.H. Coinhibitory pathways in immunotherapy for cancer. *Ann. Rev. Immunol.* **2016**, *34*, 539–573. [[CrossRef](#)]
4. Weiner, L.M.; Surana, R.; Wang, S. Monoclonal antibodies: Versatile platforms for cancer immunotherapy. *Nat. Rev. Immunol.* **2010**, *10*, 317–327. [[CrossRef](#)]
5. Clarke, J.M.; Hurwitz, H.I. Targeted inhibition of VEGF receptor 2: An update on ramucirumab. *Expert Opin. Biol. Ther.* **2013**, *13*, 1187–1196. [[CrossRef](#)] [[PubMed](#)]
6. Karlitepe, A.; Ozalp, O.; Biray, C. New approaches for cancer immunotherapy. *Tumour Biol.* **2015**, *36*, 4075–4078. [[CrossRef](#)]
7. Lobo, E.D.; Hansen, R.J.; Balthasar, J.P. Antibody pharmacokinetics and pharmacodynamics. *J. Pharm. Sci.* **2004**, *93*, 2645–2668. [[CrossRef](#)]
8. Guilleminault, L.; Lemarié, E.; Heuzé-Vourc'h, N. Monoclonal antibodies: An emerging class of therapeutics in non small cell lung cancer. *J. Cancer Ther.* **2012**, *3*, 1170–1190. [[CrossRef](#)]
9. Brennan, F.R.; Morton, L.D.; Spindeldreher, S.; Ki-essling, A.; Allenspach, R.; Hey, A.; Muller, P.Y.; Frings, W.; Sims, J. Safety and immunotoxicity assessment of immunomodulatory monoclonal antibodies. *MAbs* **2010**, *2*, 233–255. [[CrossRef](#)]
10. Hansel, T.T.; Kropshofer, H.; Singer, T.; Mitchell, J.A.; George, A.J.T. The safety and side effects of monoclonal antibodies. *Nat. Rev. Drug Discov.* **2010**, *9*, 325–338. [[CrossRef](#)]

11. Helissey, C.; Vicier, C.; Champiat, S. The development of immunotherapy in older adults: New treatments, new toxicities? *J. Geriatr. Oncol.* **2016**, *7*, 325–333. [[CrossRef](#)] [[PubMed](#)]
12. Wang, W.; Wang, E.Q.; Balthasar, J.P. Monoclonal antibody pharmacokinetics and pharmacodynamics. *Clin. Pharmacol. Ther.* **2008**, *84*, 548–558. [[CrossRef](#)]
13. Suzuki, T.; Ishii-Watabe, A.; Tada, M.; Kobayashi, T.; Kanayasu-Toyoda, T.; Kawanishi, T.; Yamaguchi, T. Importance of neonatal FcR in regulating the serum half-life of therapeutic proteins containing the Fc domain of human IgG1: A comparative study of the affinity of monoclonal antibodies and Fc fusion proteins to human neonatal FcR. *J. Immunol.* **2010**, *184*, 1968–1976. [[CrossRef](#)]
14. Ng, C.M.; Stefanich, E.; Anand, B.S.; Fielder, P.J.; Vaickus, L. Pharmacokinetics/pharmacodynamics of nondepleting anti-CD4 monoclonal antibody (TRX1) in healthy human volunteers. *Pharm. Res.* **2006**, *23*, 95–103. [[CrossRef](#)] [[PubMed](#)]
15. Hayashi, N.; Tsukamoto, Y.; Sallas, W.M.; Lowe, P.J. A mechanism-based binding model for the population pharmacokinetics and pharmacodynamics of omalizumab. *Br. J. Clin. Pharmacol.* **2007**, *63*, 548–561. [[CrossRef](#)]
16. Duan, X.; Abuqayyas, L.; Dai, L.; Balthasar, J.P.; Qu, J. High-throughput method development for sensitive, accurate, and reproducible quantification of therapeutic monoclonal antibodies in tissues using orthogonal array optimization and nano liquid chromatography/selected reaction monitoring mass spectrometry. *Anal. Chem.* **2012**, *84*, 4373–4382. [[CrossRef](#)]
17. Bronsema, K.J.; Bischoff, R.; Pijnappel, W.W.M.P.; van der Ploeg, A.T.; van de Merbel, N.C. Absolute quantification of the total and antidrug antibody-bound concentrations of recombinant human α -glucosidase in human plasma using protein G extraction and LC-MS/MS. *Anal. Chem.* **2015**, *87*, 4394–4401. [[CrossRef](#)] [[PubMed](#)]
18. An, B.; Zhang, M.; Johnson, R.W.; Qu, J. Surfactant-aided precipitation/on-pellet-digestion (sod) procedure provides robust and rapid sample preparation for reproducible, accurate and sensitive LC/MS quantification of therapeutic protein in plasma and tissues. *Anal. Chem.* **2015**, *87*, 4023–4029. [[CrossRef](#)]
19. Shen, Y.; Zhang, G.; Yang, J.; Qiu, Y.; McCauley, T.; Pan, L.; Wu, J. Online 2D-LC-MS/MS assay to quantify therapeutic protein in human serum in the presence of pre-existing antidrug antibodies. *Anal. Chem.* **2015**, *87*, 8555–8563. [[CrossRef](#)] [[PubMed](#)]
20. Wegler, C.; Gaugaz, F.Z.; Andersson, T.B.; Wiśniewski, J.R.; Busch, D.; Gröer, C.; Oswald, S.; Norén, A.; Weiss, F.; Hammer, H.S.; et al. Variability in mass spectrometry-based quantification of clinically relevant drug transporters and drug metabolizing enzymes. *Mol. Pharm.* **2017**, *14*, 3142–3151. [[CrossRef](#)] [[PubMed](#)]
21. Damen, C.W.; Derissen, E.J.; Schellens, J.H.; Rosing, H.; Beijnen, J.H. The bioanalysis of the monoclonal antibody trastuzumab by high-performance liquid chromatography with fluorescence detection after immuno-affinity purification from human serum. *J. Pharm. Biomed. Anal.* **2009**, *50*, 861–866. [[CrossRef](#)] [[PubMed](#)]
22. Todoroki, K.; Nakano, T.; Eda, Y.; Ohyama, K.; Hayashi, H.; Tsuji, D.; Min, J.Z.; Inoue, K.; Iwamoto, N.; Kawakami, A.; et al. Bioanalysis of bevacizumab and infliximab by high-temperature reversed-phase liquid chromatography with fluorescence detection after immunoaffinity magnetic purification. *Anal. Chim. Acta* **2016**, *916*, 112–119. [[CrossRef](#)] [[PubMed](#)]
23. Darwish, I.A. Immunoassay methods and their applications in pharmaceutical analysis: Basic methodology and recent advances. *Int. J. Biomed. Sci.* **2006**, *2*, 217–235.
24. Beer, P.M.; Wong, S.J.; Hammad, A.M.; Falk, N.S.; O'Malley, M.R.; Khan, S. Vitreous levels of unbound bevacizumab and unbound vascular endothelial growth factor in two patients. *Retina* **2006**, *26*, 871–876. [[CrossRef](#)]
25. AlRabiah, H.; Hamidaddin, M.A.; Darwish, I.A. Automated flow fluorescent noncompetitive immunoassay for measurement of human plasma levels of monoclonal antibodies used for immunotherapy of cancers with KinExA™ 3200 biosensor. *Talanta* **2019**, *192*, 331–338. [[CrossRef](#)]
26. Somru BioScience Inc. Cetuximab (Erbix®) PK ELISA, Catalog SBA-100-007-015. Available online: <http://www.deltaclon.com/pdf/somru/SBA-100-007-015.pdf> (accessed on 24 February 2023).
27. Darwish, I.A.; Al-Shehri, M.M.; El-Gendy, M.A. Development of new ELISA with high sensitivity and selectivity for bioanalysis of bevacizumab: A monoclonal antibody used for cancer immunotherapy. *Curr. Anal. Chem.* **2018**, *14*, 174–181. [[CrossRef](#)]
28. Al-Shehri, M.M.; El-Gendy, M.A.; Darwish, I.A. Development of specific new ELISA for bioanalysis of cetuximab: A monoclonal antibody used for cancer immunotherapy. *Curr. Pharm. Anal.* **2018**, *14*, 519–525. [[CrossRef](#)]
29. Suárez, I.; Salmerón-García, A.; Cabeza, J.; Capitán-Vallvey, L.F.; Navas, N. Development and use of specific ELISA methods for quantifying the biological activity of bevacizumab, cetuximab and trastuzumab in stability studies. *J. Chromatogr. B Anal. Technol. Biomed. Life Sci.* **2016**, *1032*, 155–164. [[CrossRef](#)]
30. Abcam Plc. Infliximab ELISA Kit, Catalog ab237647. Available online: <https://www.abcam.com/infliximab-elisa-kit-ab237647.html> (accessed on 15 December 2022).
31. Cézé, N.; Ternant, D.; Piller, F.; Degenne, D.; Azzopardi, N.; Dorval, E.; Watier, H.; Lecomte, T.; Paintaud, G. An enzyme-linked immunosorbent assay for therapeutic drug monitoring of cetuximab. *Ther. Drug Monit.* **2009**, *31*, 597–601. [[CrossRef](#)]
32. Noda, K.; Matsuda, K.; Yagishita, S.; Maeda, K.; Akiyama, Y.; Terada-Hirashima, J.; Matsushita, H.; Iwata, S.; Yamashita, K.; Atarashi, Y.; et al. A novel highly quantitative and reproducible assay for the detection of anti-SARS-CoV-2 IgG and IgM antibodies. *Sci. Rep.* **2021**, *11*, 5198. [[CrossRef](#)] [[PubMed](#)]
33. Cinquanta, L.; Fontana, D.E.; Bizzaro, N. Chemiluminescent immunoassay technology: What does it change in autoantibody detection? *Autoimmun. Highlights* **2017**, *8*, 1–8. [[CrossRef](#)] [[PubMed](#)]
34. Cai, H.H.; Chen, X. Monoclonal antibodies for cancer therapy approved by FDA. *MOJ Immunol.* **2016**, *4*, 11–12. [[CrossRef](#)]
35. Carter, P.J.; Presta, L.G. Humanized Antibodies and Methods for Making Them. U.S. Patent 6,054,297, 25 April 2000. Available online: <https://www.fda.gov/ohrms/dockets/dailys/04/sep04/090304/04e-0402-app0001-01-vol1.pdf> (accessed on 25 February 2023).

36. Generics and Biosimilars Initiative, Building Trust in Cost-Effective Treatments. Available online: <http://gabionline.net/Biosimilars/General/Biosimilars-of-cetuximab> (accessed on 25 February 2023).
37. Collin, M. Immune checkpoint inhibitors: The battle of giants. *Pharm. Pat. Anal.* **2017**, *6*, 137–139. [[CrossRef](#)] [[PubMed](#)]
38. Genentech, Inc. About Avastin: Proposed Mechanism of Action. Available online: <https://www.avastin-hcp.com/about-avastin/proposed-moa.html> (accessed on 25 February 2023).
39. Dudal, S.; Baltrukonis, D.; Crisino, R.; Goyal, M.J.; Joyce, A.; Österlund, K.; Smeraglia, J.; Taniguchi, Y.; Yang, J. Assay formats: Recommendation for best practices and harmonization from the global bioanalysis consortium harmonization team. *AAPS J.* **2014**, *16*, 194–205. [[CrossRef](#)]
40. Chen, G.; Jin, M.; Du, P.; Zhang, C.; Cui, X.; Zhang, X.; Wang, J.; Jin, F.; She, Y.; Shao, H.; et al. A review of enhancers for chemiluminescence enzyme immunoassay. *Food Agric. Immunol.* **2017**, *28*, 315–327. [[CrossRef](#)]
41. Karatani, H. Luminol–hydrogen peroxide–horseradish peroxidase chemiluminescence intensification by kosmotrope ammonium sulfate. *Anal. Sci.* **2022**, *38*, 613–621. [[CrossRef](#)]
42. Yang, L.; Jin, M.; Du, P.; Chen, G.; Zhang, C.; Wang, J.; Jin, F.; Shao, H.; She, Y.; Wang, S.; et al. Study on enhancement principle and stabilization for the luminol-H₂O₂-HRP chemiluminescence system. *PLoS ONE* **2015**, *10*, e0131193. [[CrossRef](#)]
43. Dong, B.; Fan, Q.; Li, M.; Huan, Y.; Feng, G.; Shan, H.; Fei, Q. Determination of tyrosine by sodium fluorescein-enhanced ABEI-H₂O₂-horseradish peroxidase chemiluminescence. *J. Anal. Sci. Technol.* **2021**, *21*, 16. [[CrossRef](#)]
44. Dotsikas, Y.; Loukas, Y.L. Employment of 4-(1-imidazolyl)phenol as a luminol signal enhancer in a competitive-type chemiluminescence immunoassay and its comparison with the conventional antigen–horseradish peroxidase conjugate-based assay. *Anal. Chim. Acta* **2004**, *509*, 103–109. [[CrossRef](#)]
45. Dotsikas, Y.; Yannis, L.L. Effect of the luminol signal enhancer selection on the curve parameters of an immunoassay and the chemiluminescence intensity and kinetics. *Talanta* **2007**, *71*, 906–910. [[CrossRef](#)]
46. García Campaña, A.M.; Baeyens, W.R.G. *Chemiluminescence in Analytical Chemistry*; Marcel Dekker: New York, NY, USA, 2001; p. 177.
47. The International Council for Harmonization (ICH). *Q2(R1) on Validation of Analytical Procedure*; ICH: Geneva, Switzerland, 2022.
48. Bender, J.L.; Adamson, P.C.; Reid, J.M.; Xu, L.; Baruchel, S.; Shaked, Y.; Kerbel, R.S.; Cooney-Qualter, E.M.; Stempak, D.; Chen, H.X.; et al. Phase I trial and pharmacokinetic study of bevacizumab in pediatric patients with refractory solid tumors: A children’s oncology group study. *J. Clin. Oncol.* **2008**, *26*, 399–405. [[CrossRef](#)] [[PubMed](#)]
49. Findlay, J.W.; Smith, W.C.; Lee, J.W.; Nordblom, G.D.; Das, I.; DeSilva, B.S.; Khan, M.N.; Bowsher, R.R. Validation of immunoassays for bioanalysis: A pharmaceutical industry perspective. *J. Pharm. Biomed. Anal.* **2000**, *21*, 1249–1273. [[CrossRef](#)] [[PubMed](#)]

Disclaimer/Publisher’s Note: The statements, opinions and data contained in all publications are solely those of the individual author(s) and contributor(s) and not of MDPI and/or the editor(s). MDPI and/or the editor(s) disclaim responsibility for any injury to people or property resulting from any ideas, methods, instructions or products referred to in the content.